Bioorganic & Medicinal Chemistry Letters 20 (2010) 5781–5786

Contents lists available at ScienceDirect

Bioorganic & Medicinal Chemistry Letters

journal homepage: www.elsevier.com/locate/bmcl

Novel bisphosphonate inhibitors of the human farnesyl pyrophosphate synthase

Joris W. De Schutter [a], Serge Zaretsky [a,†], Sarah Welbourn [b], Arnim Pause [b], Youla S. Tsantrizos [a,b,*]

[a] Department of Chemistry, McGill University, Montreal, Quebec, Canada H3A 2K6
[b] Department of Biochemistry, McGill University, Montreal, Quebec, Canada H3G 1Y6

ARTICLE INFO

Article history:
Received 12 July 2010
Accepted 30 July 2010
Available online 11 August 2010

Keywords:
Bisphosphonates
Human FPPS

ABSTRACT

A structure-based approach was pursued in designing novel bisphosphonate inhibitors of the human farnesyl pyrophosphate synthase (hFPPS). Preliminary SAR and structural evidence for the simultaneous binding of these inhibitors into the isopentenyl pyrophosphate (IPP) and the geranyl pyrophosphate (GPP) substrate sub-pockets of the enzyme are presented.

The human farnesyl pyrophosphate synthase (hFPPS) is responsible for the catalytic elongation of dimethylallyl pyrophosphate (DMAPP) to geranyl pyrophosphate (GPP) and then to farnesyl pyrophosphate (FPP) via the successive condensation of two isopentenyl pyrophosphate (IPP) units. FPP is the key biosynthetic precursor to geranylgeranyl pyrophosphate (GGPP), a transformation in the mevalonate pathway that is catalyzed by the human geranylgeranyl pyrophosphate synthase (hGGPPS). Post-translational prenylation of proteins with either FPP or GGPP is estimated to constitute approximately 2% of the total mammalian proteome.[1] These post translational modifications confer membrane localization, promote specific protein–protein interactions and play a crucial role in controlling intracellular trafficking, cell signaling and cell proliferation in various human cancers.

Over the last 15 years, interest in hFPPS inhibitors focused mainly on the role of this enzyme in protein prenylation in osteoclasts.[2–4] Nitrogen-containing bisphosphonate (*N*-BP) inhibitors of hFPPS are currently used in the treatment of osteoporosis, tumor-induced hypercalcemia, Paget's disease and osteolytic metastases.[5] However, increasing awareness of the pleiotropic affects that hFPPS inhibitors have in human diseases (including various types of cancers), has stimulated investigations into potential therapeutics that target this enzyme. The antitumor effects of hFPPS inhibitors may be due to a direct impact on oncogenic proteins or yet unclear indirect effects involving the immune system.[6–11]

The drugs alendronate (**1**, Fosamax®), zoledronate (**2**, Zometa®) and risedronate (**5**, Actonel®), and the more recently reported analogues **3**, **4** and **6**–**10** typify the molecular architectures of currently known bisphosphonates.[1–4,12,13] The main pharmacophore anchoring these inhibitors to the hFPPS active site is the bisphosphonate moiety, which coordinates with the aspartate-rich fingerprint region via chelation of three Mg^{2+} ions. Consequently, the selectivity for hFPPS versus other structurally related human enzymes, such as hGGPPS, decaprenyl diphosphate synthase (hDPPS) and squalene synthase (hSQS) is usually poor to modest. For example, stronger inhibition of hSQS than hFPPS was recently reported for analogs **3** and **4**,[13] whereas analog **9** was found to inhibit hFPPS, hGGPPS and hDPPS with almost equal potency.[14] In contrast, compound **10** was reported to be somewhat selective for hGGPPS, exhibiting a selectivity index of approximately 47 and 17 for hGGPPS/hFPPS and hGGPPS/hDPPS, respectively.[14]

In addition to the bisphosphonate pharmacophore, binding of compounds such as **2** and **5** into the GPP sub-pocket of the enzymes is biased by favorable hydrogen-bond interactions between their protonated heterocyclic side chain and residues Lys 214 and Thr 215 (Fig. 1a). The importance of the pyridine side chain and the proper alignment between the protonated nitrogen atom and residues Lys 214/Thr 215 (in the presumed bound state) were previously reported by Dunford et al.[4] In order to explore the SAR of pyridine derivatives that could simultaneously occupy both the GPP- and IPP- sub-pockets of the active site, novel derivatives were designed that do not require protonation for binding. To facilitate our investigation, previously reported protocols for the preparation of bisphosphonates were also modified and rendered amenable to the parallel synthesis of our inhibitors.

Modeling studies: Numerous crystal structures of hFPPS-bound to its substrates and/or inhibitors have been reported; these include the complexes of enzyme-bound **5** (e.g., PDB codes 1YQ7, 1YV5) and the ternary complexes of **2** and IPP simultaneously bound to the enzyme (PDB code 1ZW5). Mindful of the large

* Corresponding author. Address: Department of Biochemistry, McGill University, 801 Sherbrooke Street, West Montreal, Quebec, Canada H3A 2K6. Tel.: +1 514 398 3638; fax: +1 514 398 3797.
E-mail address: Youla.tsantrizos@mcgill.ca (Y.S. Tsantrizos).
† Undergraduate research participant.

0960-894X/$ - see front matter © 2010 Elsevier Ltd. All rights reserved.
doi:10.1016/j.bmcl.2010.07.133

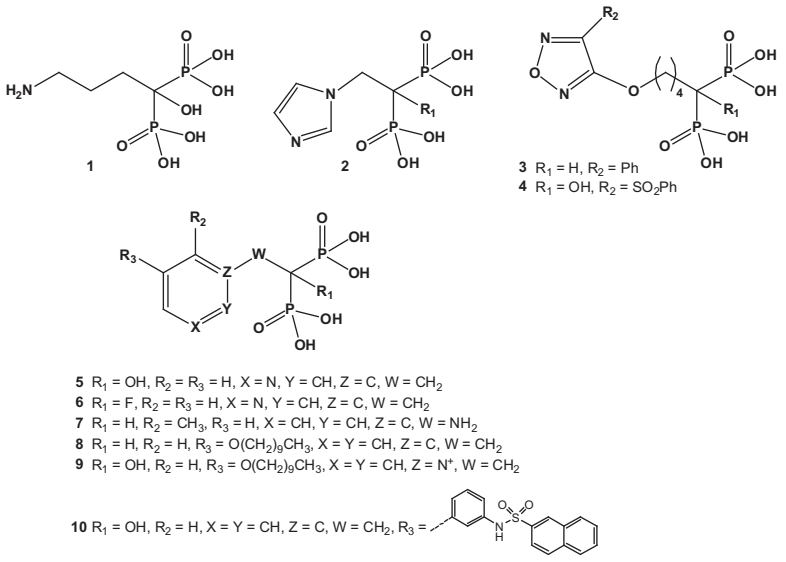

conformational changes that are induced to the C-terminal region of the protein upon binding of IPP and an inhibitor, as well as the essential role of the C-terminal residues ^{350}KRRK^{353} for catalytic activity, we chose to develop an in silico model based on the crystal structure of the hFPPS-IPP-**2** complex (1ZW5).[15,16] Initially, a small set of >200 virtual pyridine-based molecules were docked in to the hFPPS active site using GLIDE (version 5.5, Shrödinger, LLC, New York, NY 2009; standard parameters of XP-mode were used); a sub-set of these compounds is shown in Table 1. The bisphosphonate was considered fully ionized and the pyridine nitrogen protonated to attain the interactions with Lys 214 and Thr 215. As it would be expected, when a large substituent was attached to the pyridine ring, these derivatives were not able to adopt the expected bound orientation in the GPP-pocket, or engage in interactions with Lys 214 and Thr 215. All derivatives were also docked with a neutral pyridine side chain. In the latter case, more than 80 analogs from those shown in Table 1 could bind into the IPP sub-pocket, placing the pyridine moiety approximately 90° from that of the enzyme-bound side chain of **5** (Fig. 1b). The docking score assigned by GLIDE (gscore) was used only as a qualitative measure and assessment of favorable binding was based primarity on visual inspection of the output poses. Proper alignment between the bisphosponate moiety and the Mg^{2+} ions, and favorable/unfavorable potential ligand–protein interactions, were considered. A sub-set of 16 analogs, including **11h**, **11l**, **11m** and **13b** which were predicted to be inactive (i.e. GLIDE did not generate an output pose for these compounds or the bisphosphonate moiety was misposed) was synthesized, in order to validate our approach.

Synthetic studies: Analogs of scaffold **11** were prepared starting from the chloro or bromo nitropyridine **18** (Scheme 1). Suzuki cross-coupling of **18** with heterocyclic (Het) boronic acids, followed by catalytic hydrogenation of the nitro group produced intermediates **19** in 30–80% overall yield. Conversion of anilines **19** to the bisphosphonate esters was achieved by condensation with diethyl phosphite and triethyl orthoformate at high temperatures as previously reported.[17] Deprotection of the ethyl esters was performed by transesterification with bromotrimethylsilane, followed by hydrolysis of the silyl esters with methanol.[18] Although this reaction proceeds very slowly (incomplete conversion even

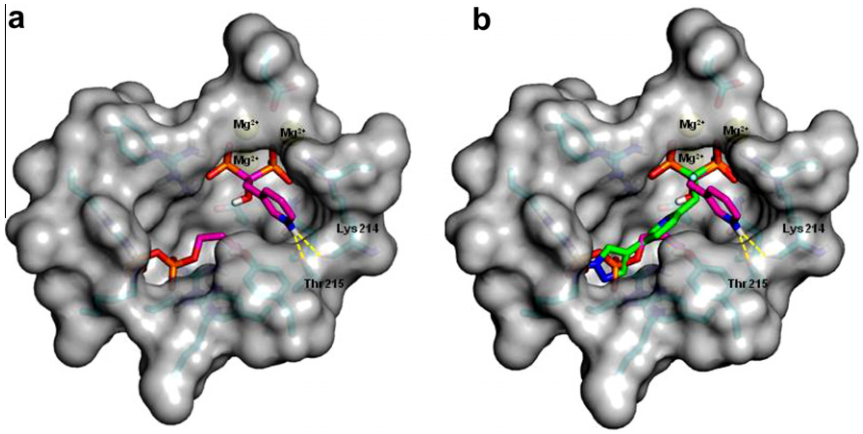

Figure 1. Semitransparent protein surface of the hFPPS active site (some residues were removed for clarity). The three Mg^{2+} ions mediating interactions with the bisphosphonate moiety are highlighted. The IPP substrate and the bound inhibitors are shown in stick form. The carbon backbone of IPP and **5** are highlighted in magenta and inhibitor **13f** in green colour. Oxygen, nitrogen and phosphorus atoms are coloured in red, blue and orange, respectively. Hydrogen-bond interactions between the protonated heterocyclic side chain of **5** and residues Lys 214/Thr 215 are indicated with dashed yellow lines. (a) Model of an hFPPS-IPP-**5** ternary complex, based on the crystal structure of hFPPS-IPP-**2** (PDB 1ZW4) and hFPPS-**5** (PDB 1YV5); (b) analog **13f** superimposed with IPP in the hFPPS-IPP-**5** complex.

Table 1
Virtual library of potential hFPPS inhibitors

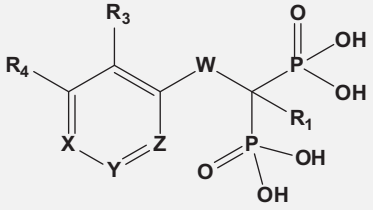

11: R_1 = H, R_3 = R_4 = H, W = NH, X = C-Het, Y = N, Z = CH
12: R_1 = F, R_3 = R_4 = H, W = CH_2, X = CH, Y = C-Het, Z = N
13: R_1 = F, R_3 = R_4 = H, W = CH_2, X = C-Het, Y = CH, Z = N
14: R_1 = F, R_3 = H, R_4 = Het, W = CH_2, X = Y = CH, Z = N
15: R_1 = F, R_3 = H, R_4 = Het, W = CH_2, X = Z = CH, Y = N
16: R_1 = F, R_3 = R_4 = H, W = CH_2, X = C-Het, Y = N, Z = CH
17: R_1 = F, R_3 = H, R_4 = Het, W = CH_2, X = N, Y = Z = CH
5: R_1 = OH, R_3 = R_4 = H, X = Z = CH, Y = N, W = CH_2
25: R_1 = OH, R_3 = R_4 = H, X = Z = Y = CH, W = CH_2

Het=

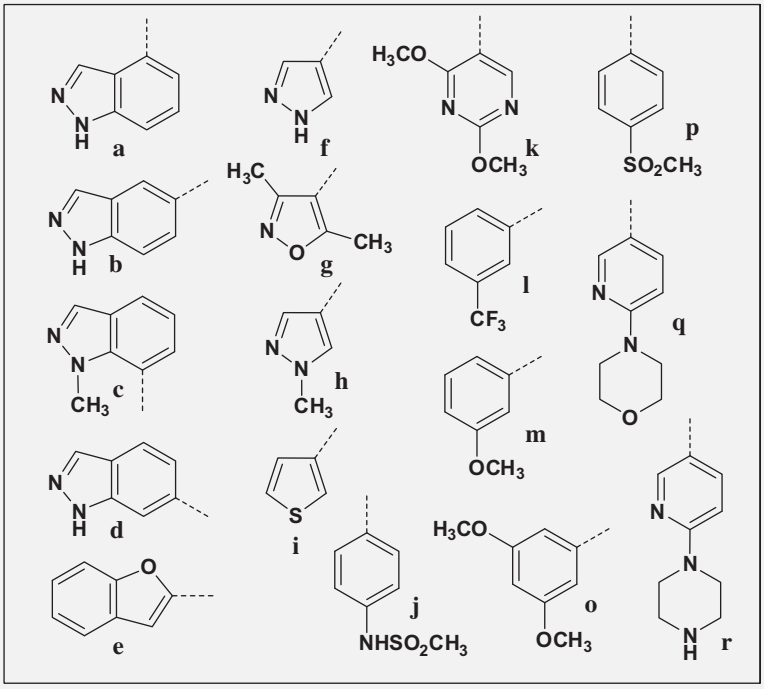

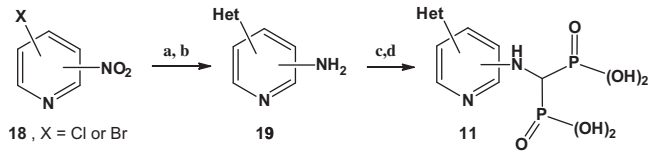

Scheme 1. Reagents and conditions: (a) Het-$B(OH)_2$, 10% $Pd(PPh_3)_4$, 2 M Na_2CO_3, DME, 80 °C; (b) H_2, Pd/C, EtOAc, rt; (c) $HP(O)(OEt)_2$, $CH(OEt)_3$, 110 °C; (d) (i) excess TMBS, DCM; (ii) MeOH.

after 48 h at rt), it allowed for isolation of the pure final products **11** by simple precipitation (25–65% isolated yield).

The synthesis of analogs corresponding to scaffolds **12**–**17** (Table 1, Scheme 2) was initiated with the appropriately substituted halo picolinic, nicotinic or isonicotinic acid (**20**), which was first converted to the corresponding mixed anhydride with ethylchloroformate, reduced with $NaBH_4$ to give the alcohol **21** and then

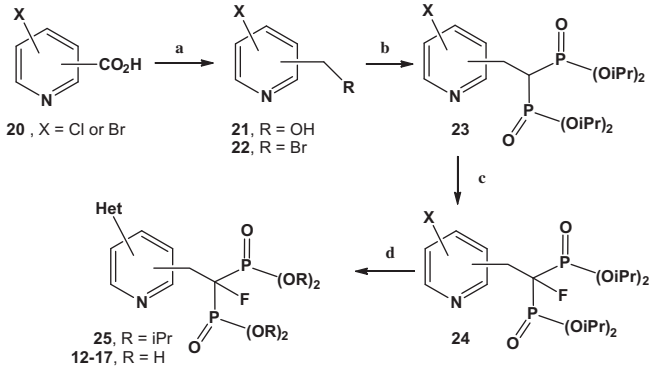

Scheme 2. Reagents and conditions: (a) (i) ethylchloroformate, NEt_3, THF, 0 °C; (ii) $NaBH_4$, H_2O; (iii) PBr_3, DCM, 0 °C to rt; (b) $CH_2[PO(OiPr)_2]_2$, NaH, DMF, 0 °C to rt; (c) NFSI, *n*BuLi, THF, −78 °C to rt; (d) (i) Het-$B(OH)_2$, 10% $Pd(PPh_3)_4$, 2 M Na_2CO_3, DME, 80 °C, 17 h (bromopyridines) or 110 °C for 10 min in a microwave (chloropyridines); (ii) 6 M HCl, 100 °C.

treated with PBr_3 to obtain the intermediate bromide **22**; yield for the formation of both **21** and **22** ranged from 50% to 90%. Deprotonation of tetraisopropyl methylenebis(phosphonate) with sodium hydride, followed by substitution of the bromide moiety of **22**,[3] produced the key building block **23** in yields of 30–60%. Fluorination at Cα to the phosphonates using the conditions previously reported by McKenna and co-workers failed for these compounds.[3] However, intermediate **24** was successfully obtained using *N*-fluoro-*N*-(phenylsulfonyl)benzenesulfonamide (NFSI) as the fluorinating agent under strongly basic conditions. Interestingly, the yields of this reaction were modest (30–40%) for all analogs with a *para*-substituted pyridine ring (i.e. halide precursors to scaffolds **13** and **16**), irrespective of the position of the pyridine nitrogen, whereas, good to excellent yields (70–90%) were obtained with the *meta*-substituted scaffolds. Suzuki cross-coupling of **24** with a heterocyclic (Het) boronic acid produced the bisphosphonate esters **25** in 30–70% yield. Hydrolysis of the bisphosphonate ester **25** in 6 N HCl, followed by treatment with NaOH led to the formation of the monosodium salt of each analog **12**–**17**, which was purified by C_{18} reversed phase chromatography to give white or pale yellow solids (50–75% overall yield).

Human FPPS inhibition and preliminary SAR: A clone encoding the human recombinant FPPS enzyme with an *N*-terminal His_6-tag (vector p11; SGC Oxford) was expressed in *Escherichia coli* and

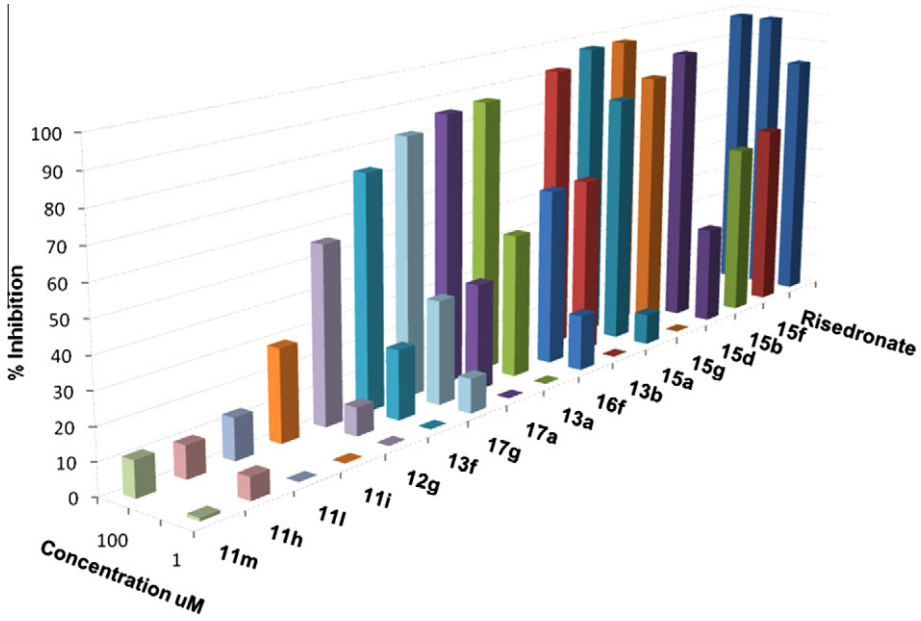

Figure 2. Inhibition of hFPPS at 1, 10 and 100 μM concentrations of each new analog.

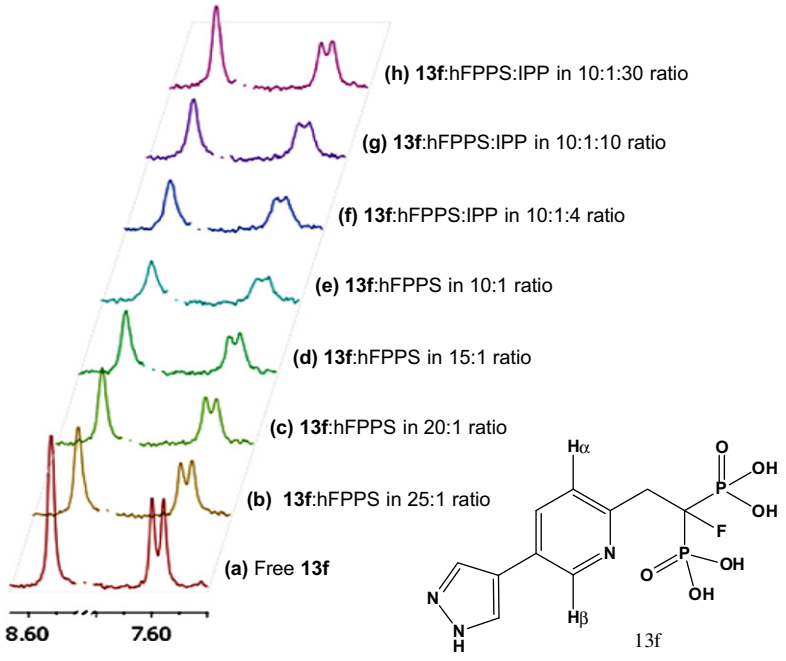

Figure 3. Section of the ^1H NMR spectra of inhibitor **13f** corresponding to the Hα and Hβ resonances at δ 7.59 and 8.58, respectively. The composition of each sample is indicated.

purified as previously described by Dunford,[4] Oppermann,[16] and co-workers. For this preliminary evaluation of our compounds, the enzyme was only partly purified (the final gel filtration on a Superdex 200 column was omitted).[4,16] The hFPPS activity was measured using similar assay conditions to those reported by Dunford et al. (pre-incubation period was reduced to 5 min instead of 10 min).[4] Initially, the potential of all compounds to inhibit hFPPS was evaluated at the concentration of 1 μM (Fig. 2). For the purpose of validating our in silico studies, some analogs were also tested at 10 and 100 μM concentrations (Fig. 2). Although the energy scores computed by GLIDE were based on a rigid protein model, overall, a good correlation was observed between the computational predictions and experimental data (Fig. 2). Potency comparison between analogs having the same Het substituent, but different pyridine cores (i.e. **11**–**17**) suggests that scaffold **15** provides some advantages. For example, analog **15a** (81% inhibition at 10 μM) is more potent than analogs **13a** and **17a** (46% and 34% inhibition at 10 μM, respectively), and similarly **15g** (86% inhibition at 10 μM) is more potent than **12g** and **17g** (9% and 33% inhibition at 10 μM, respectively). Two analogs, **15b** and **15f**, were identified that exhibited an inhibition value of >50% at concentration of 1 μM. Concentration dependent inhibition of hFPPS was observed for both **15f** and **15b** and IC_{50} values of 650 and 700 nM, respectively, were calculated; under the same assay conditions, the IC_{50} of **5** was ~300 nM.

NMR studies: Based on the available structural data and our in silico model, it is reasonable to assume that the potency of **15b** and **15f** is derived from interactions with the hFPPS active site that are different from those observed with risedronate (**5**). In order to probe the binding mode of our inhibitors, competition experiments were conducted using ^{1}H line broadening NMR.[19,20] Broadening of the ^{1}H resonances of compound **13f** was observed in the presence of hFPPS, confirming binding of **13f** to the enzyme; free state of **13f** (Fig. 3a) versus enzyme-bound **13f** in fast exchange with its free state (Fig. 3b–e). Addition of IPP to the hFPPS/**13f** NMR sample restored the ^{1}H resonances of **13f** almost completely (Fig. 3h). These results strongly suggest that IPP and **13f** compete for binding into the same sub-pocket of the active site (Fig. 1b). The proposed binding mode is in clear contrast to those of **2** and **5** which are known to bind mostly in the GPP sub-pocket and can form ternary complexes with IPP (Fig. 1a vs b). A direct competition experiment with analogs **15b** or **15f** and IPP cannot be easily performed, due to the high affinity of these inhibitors for the enzyme. However, the size and shape of these compounds would clearly forbid binding to the GPP sub-pocket without imposing a dramatic conformational rearrangement to the protein structure. Displacement of the hFPPS-bound **13f** (i.e. reversal of line broadening in the ^{1}H NMR spectrum of **13f**) could also be achieved with risedronate (**5**), strongly supporting that **13f** also binds (at least in part) to the GPP sub-pocket of the enzyme. Our NMR data is consistent with the model developed from our docking studies for **13f** and the more potent structurally related analogs **15b** and **15f** (Fig. 1b).

In summary, a small library of virtual molecules was docked into the active site of hFPPS. The protein structure of the hFPPS-IPP-**2** complex, which has the C-terminal residues conformationally rigidified and sequestering the active site from bulk solvent, was used to develop a model for the plausible ternary complex of hFPPS-IPP-**5**. We reasoned that the binding orientation of **5** is biased by the favorable interactions attained with residues Lys 214 and Thr 215 upon protonation of its pyridine side chain. These interactions are limiting the binding of **5** into the GPP sub-pocket and may restrict SAR optimization into more potent and selective inhibitors. To test this hypothesis, we selected in silico new pyridine-based derivatives that could bind to hFPPS without protonation and could simultaneously occupy both the IPP and the GPP sub-pockets of the active site. A small set of compounds was synthesized, including analogs **15b** and **15f** which exhibit comparable in vitro potency to **5**. Docking and ^{1}H line broadening NMR data strongly suggest that the binding mode of these compounds is distinctly different from that of **5** and does not rely on interactions with residue Lys 214. However, based on our docking data, the neutral pyridine nitrogen of the enzyme-bound **15b** or **15f** is close enough to the hydroxyl side chain of Thr 215 to act as a hydrogen-bond acceptor. Comparison of the inhibition observed with analogs having the same Het substituent but different pyridine cores strongly suggests that scaffold **15** provides some advantages over the others. The novel analogs **15b** and **15f** (which, *arguably*, should not be compared to **5** in terms of their IC_{50} values) represent promising new leads for further optimization.

Acknowledgments

We wish to thank Professor Nicolas Moitessier and Dr. Eric Therrien for their contributions to the computational studies (Chemistry Department, McGill University). We are grateful to Dr. James Dunford (The Botnar Research Centre, The Institute of Musculoskeletal Sciences University of Oxford Nuffield Orthopaedic Centre) for his valuable advice on the set-up of the hFPPS assay. We also wish to thank Dr. Tara Sprules for assistance with the set-up of the ^{1}H Line broadening NMR experiments, which were acquired on a 500 MHz NMR instrument at the Québec/Eastern Canada High Field NMR Facility, supported by the Natural Sciences and Engineering Research Council of Canada, the Canada Foundation for Innovation, the Québec ministère de la recherche en science et technologie, and McGill University. We gratefully acknowledge the financial support of McGill University and the Natural Sciences and Engineering Research Council of Canada (NSERC), the Canadian Institute of Health Research (CIHR) and the Groupe de Recherche Axé sur la Structure des Protéines (GRASP).

References and notes

1. Nguyen, U. T. T.; Guo, Z.; Delon, C.; Wu, Y.; Deraeve, C.; Fränzel, B.; Bon, R. S.; Blankenfeldt, W.; Goody, R. S.; Waldmann, H.; Wolters, D.; Alexandrov, K. *Nat. Chem.* **2009**, *5*, 227.
2. Dunford, J. E.; Thompson, K.; Coxon, F. P.; Luckma, S. P.; Hahn, F. M.; Poulter, C. D.; Ebetino, F. H.; Rogers, M. J. *J. Pharmacol. Exp. Ther.* **2001**, *296*, 235.
3. Marma, M. S.; Xia, Z.; Stewart, C.; Coxon, F.; Dunford, J. E.; Baron, R.; Kashemirov, B. A.; Ebetino, F. H.; Triffitt, J. T.; Russell, G. G.; McKenna, C. E. *J. Med. Chem.* **2007**, *50*, 5967.
4. Dunford, J. E.; Kwaasi, A. A.; Rogers, M. J.; Barnett, B. L.; Ebetino, F. H.; Russell, R. G. G.; Oppermann, U.; Kavanagh, K. L. *J. Med. Chem.* **2008**, *51*, 2187.
5. Review: Caraglia, M.; Santini, D.; Marra, M.; Vincenzi, B.; Tonini, G.; Budillon, A. *Endocr. Relat. Cancer* **2006**, *13*, 7.
6. Oldfield, E. *Acc. Chem. Res.* **2010**, xxxx.
7. Gnant, M.; Mlineritsch, B.; Schippinger, W.; Luschin-Ebengreuth, G.; Pöstlberger, S.; Menzel, C.; Jakesz, R.; Seifert, M.; Hubalek, M.; Bjelic-Radisic, V.; Samonigg, H.; Tausch, C.; Eidtmann, H.; Steger, G.; Kwasny, W.; Dubsky, P.; Fridrik, M.; Fitzal, F.; Stierer, M.; Rücklinger, E.; Greil, R. *N. Eng. J. Med.* **2009**, *360*, 679.
8. Dieli, F.; Vermijlen, D.; Fulfaro, F.; Caccamo, N.; Meraviglia, S.; Cicero, G.; Roberts, A.; Buccheri, S.; D'Asaro, M.; Gebbia, N.; Salerno, A.; Eberl, M.; Hayday, A. C. *Cancer Res.* **2007**, *67*, 7450.
9. Wihelm, M.; Kunzmann, V.; Eckstein, S.; Reimer, P.; Weissinger, F.; Ruediger, T.; Tony, H.-P. *Blood* **2003**, *102*, 200.
10. Greenwood, J.; Steinman, L.; Zamvil, S. S. *Nat. Rev. Immunol.* **2006**, *6*, 358.
11. Morita, C. T.; Jin, C.; Sarikonda, G.; Wang, H. *Immunol. Rev.* **2007**, *215*, 59.
12. Zhang, Y.; Cao, R.; Yin, F.; Hudock, M. P.; Guo, R.-T.; Krysiak, K.; Mukherjee, S.; Gao, Y.-G.; Robinson, H.; Song, Y.; No, J. H.; Bergan, K.; Leon, A.; Cass, L.; Goddard, A.; Chang, T.-K.; Lin, F.-Y.; Van Beek, E.; Papapoulos, S.; Wang, A. H.-J.; Kubo, T.; Ochi, M.; Mukkamala, D.; Oldfield, E. *J. Am. Chem. Soc.* **2009**, *131*, 5153.
13. Lolli, M. L.; Rolando, B.; Tosco, P.; Chaurasia, S.; Di Stilo, A.; Lazzarato, L.; Gorassini, E.; Ferracini, R.; Oliaro-Bosso, S.; Fruttero, R.; Gasco, A. *Bioorg. Med. Chem.* **2010**, *18*, 2428.
14. Zhang, Y.; Cao, R.; Yin, F.; Lin, F.-Y.; Wang, H.; Krysiak, K.; No, J.-H.; Mukkamala, D.; Houlihan, K.; Li, J.; Morita, C. T.; Oldfield, E. *Angew Chem., Int. Ed.* **2010**, *49*, 1136.
15. Rondeau, J.-M.; Bitsch, F.; Bourgier, E.; Geiser, M.; Hemmig, R.; Kroemer, M.; Lehmann, S.; Ramage, P.; Rieffel, S.; Strauss, A.; Green, J. R.; Jahnke, W. *ChemMedChem* **2006**, *1*, 267.

16. Kavanagh, K. L.; Guo, K.; Dunford, J. E.; Wu, X.; Knapp, S.; Ebetino, F. H.; Rogers, M. J.; Russell, R. G. G.; Oppermann, U. *Proc. Natl. Acad. Sci. U.S.A.* **2006**, *103*, 7829.
17. Martin, M. B.; Grimley, J. S.; Lewis, J. C.; Heath, H. T., III; Bailey, B. N.; Kendrick, H.; Yardley, V.; Caldera, A.; Lira, R.; Urbina, J. A.; Moreno, S. N. J.; Docampo, R.; Croft, S. L.; Oldfield, E. *J. Med. Chem.* **2001**, *44*, 909.
18. Jiang, Q.; Yang, L.; Hai, L.; Wu, Y. *Lett. Org. Chem.* **2008**, *5*, 229.
19. Ni, F. *Prog. Nucl. Magn. Reson. Spectrosc.* **1994**, *26*, 517.
20. Tsantrizos, Y. S.; Bolger, G.; Bonneau, P.; Cameron, D. R.; Goudreau, N.; Kukolj, G.; LaPlante, S. R.; Llinas-Brunet, M.; Nar, H.; Lamarre, D. *Angew Chem., Int. Ed.* **2003**, *42*, 1355.